HHS Public Access

Author manuscript

Free Radic Biol Med. Author manuscript; available in PMC 2021 February 01.

Published in final edited form as:

Free Radic Biol Med. 2020 February 01; 147: 102–113. doi:10.1016/j.freeradbiomed.2019.12.015.

The HIV-Tat protein interacts with Sp3 transcription factor and inhibits its binding to a distal site of the *sod2* promoter in human pulmonary artery endothelial cells

Terrin L. Manes[a,*], **Ari Simenauer**[a,*], **Jason L. Geohring**[a], **Juliana Flemming**[a], **Michael Brehm**[b], **Adela Cota-Gomez**[a]

[a]University of Colorado Anschutz Medical Campus, Department of Medicine Division of Pulmonary Sciences and Critical Care Medicine, 12700 E. 19th Avenue, Mailstop C272, Aurora, CO 80045

[b]University of Massachusetts Medical School, 368 Plantation Street, AS7-2053, Worcester, MA 01605

Abstract

Redox imbalance results in damage to cellular macromolecules and interferes with signaling pathways, leading to an inflammatory cellular and tissue environment. As such, the cellular oxidative environment is tightly regulated by several redox-modulating pathways. Many viruses have evolved intricate mechanisms to manipulate these pathways for their benefit, including HIV-1, which requires a pro-oxidant cellular environment for optimal replication. One such virulence factor responsible for modulating the redox environment is the HIV Transactivator of transcription (Tat). Tat is of particular interest as it is actively secreted by infected cells and internalized by uninfected bystander cells where it can elicit pro-oxidant effects resulting in inflammation and damage. Previously, we demonstrated that Tat regulates basal expression of Superoxide Dismutase 2 (*sod2)* by altering the binding of the Sp-transcription factors at regions relatively near (approx. −210 nucleotides) upstream of the transcriptional start site. Now, using *in silico* analysis and a series of *sod2* promoter reporter constructs, we have identified putative clusters of Sp-binding sites located further upstream of the proximal *sod2* promoter, between nucleotides −3400 to −210, and tested their effect on basal transcription and for their sensitivity to HIV-1 Tat. In this report, we demonstrate that under basal conditions, maximal transcription requires a cluster of Sp-binding sites in the −584 nucleotide region, which is extremely sensitive to Tat. Using chromatin immunoprecipitation (ChIP) we demonstrate that Tat results in altered occupancy of Sp1 and Sp3 at this distal Tat-sensitive regulatory element and strongly stimulated endogenous expression of SOD2 in human pulmonary artery endothelial cells (HPAEC). We also report altered expression of Sp1 and Sp3 in Tat-expressing HPAEC as well as in the lungs of

Declaration of interest: none

Corresponding author: Adela Cota-Gomez, Ph.D., Adela.Cota-Gomez@cuanschutz.edu, Phone: 303-724-6085.

*Co-first authors with equal contribution

HIV-1 infected humanized mice. Lastly, Tat co-immunoprecipitated with endogenous Sp3 but not Sp1 and did not alter the acetylation state of Sp3. Thus, here, we have defined a novel and important cis-acting factor in HIV-1 Tat-mediated regulation of SOD2, demonstrated that modulation of Sp1 and Sp3 activity by Tat promotes SOD2 expression in primary human pulmonary artery endothelial cells and determined that pulmonary levels of Sp3 as well as SOD2 are increased in the lungs of a mouse model of HIV infection.

Graphical Abstract

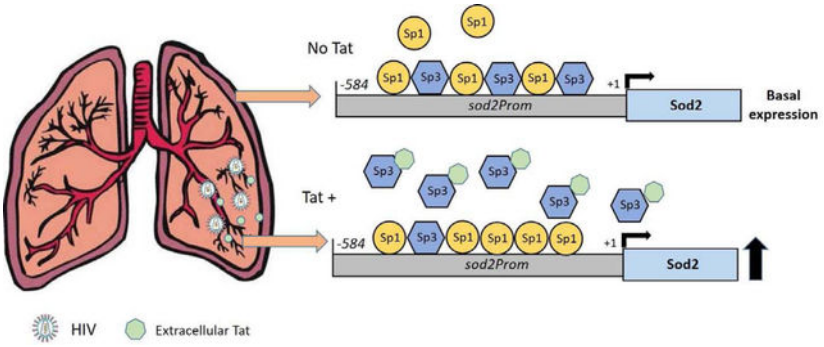

Introduction

Cellular and systemic oxidative stress is an established consequence of HIV infection, and while modern anti-retroviral therapy has been widely successful in mitigating the AIDS epidemic, HIV patients remain chronically infected and exhibit biomarkers of increased oxidative stress. Accordingly, HIV infected patients are at a dramatically increased risk of systemic inflammatory diseases, and the chronic oxidative stress elicited by HIV infection is thought to be a driving factor of these pathologies[1,2]. While a number of viral factors have been implicated in these pro-oxidant processes, the molecular mechanisms by which they evoke such oxidative biological environments remain relatively thinly researched. However, an early clue in the field of HIV related oxidative stress came with the observation that the HIV Transactivator of Transcription (Tat) downregulated expression of the Manganese-containing Superoxide Dismutase, SOD2 [3]. Tat is an early HIV gene that is responsible for transactivation of viral gene transcription from the long terminal repeat of integrated proviral DNA and is therefore integral to the life cycle of the virus [4,5]. Interestingly, Tat is secreted from infected cells into the extracellular environment where it is internalized by uninfected bystander cells and is known to interfere with cellular function by modulating a number of transcriptional pathways [6,7]. In this capacity, Tat acts as a bridge linking HIV infected cells to the larger extracellular environment.

SOD2 is a mitochondrial antioxidant enzyme that is integral to the maintenance of cellular redox homeostasis by way of catalyzing the conversion of the highly potent ROS, superoxide ($O_2^{\cdot}$), to hydrogen peroxide and diatomic oxygen. Mutations in the *sod2* gene are associated with a wide array of diseases including cancer respiratory, cardiovascular and neurodegenerative diseases [8–10]. Furthermore, it has been demonstrated that mutant mice lacking SOD2 die as neonates due to cardiomyopathy and oxidative mitochondrial injury,

and that overexpression of the cytosolic CuZnSOD in these mice could not compensate for the loss of SOD2 [11]. As such, the observation that Tat repressed SOD2 expression warranted further research into the mechanisms governing this response. Transcriptional regulation of SOD2 is cell-specific and sensitive to a number of exogenous factors including oxidative stress and inflammation [12]. The human *sod2* promoter sequences immediately flanking the transcription initiation site contain a TATA-less region of high GC content with multiple Sp and AP binding sites [13]. Xu et al demonstrated this region constitutes the basal *sod2* promoter, and that Sp factors are important regulators of *sod2* expression. They determined the relative basal transcriptional activity of constructs extending upstream of −210 nucleotides and found that a construct extending out to −555 nucleotides exhibited maximal transcription, 2-fold higher than the −210 construct, and that there was no more increase in transcriptional activity with any fragment extending beyond −555 nucleotides. Subsequently, we demonstrated that Tat regulated basal *sod2* promoter activity by altering the binding activity of transcription factors Sp1 and Sp3 to the proximal promoter region (−73 to −123 nucleotides) [14]. Furthermore, in a Tat transgenic mouse line, we observed increase biomarkers of oxidative stress as well as lung cellular infiltrate, though overall SOD2 was increased, suggesting a compensatory physiological response to Tat mediated injury [15].

Previous work attempting to elucidate the mechanisms by which Tat modulates SOD2 has relied on transformed cell lines as well as Sp1/Sp3 deficient *drosophila* S2 cells and focuses only on the proximal promoter region, −210 nucleotides from the transcriptional start site. Here, in an effort to further characterize Tat mediated basal regulation of *sod2*, we performed an *in-silico* analysis of the sequences further upstream of the human *sod2* proximal promoter, between nucleotides −3406 to −210 from the transcriptional start. We found several clusters of Sp binding sites of varying strengths (Fig.1) and hypothesized that, as with the Sp clusters contained in the −210 region, these distal sites are also regulated by Tat. In a physiologically relevant cell system, primary human pulmonary arterial endothelial cells (HPAEC), we determined the effects of Tat on transcription from these distal Sp-binding clusters. In this report, we demonstrate that a cluster of Sp binding sites located near the −584 region is required for maximal transcription and is exquisitely sensitive to Tat. Thus, this distal Tat-sensitive site (DTSS) is an important cis-acting factor in Tat-mediated *sod2* regulation in HPAEC. We also show that in HPAEC, Tat alters the binding pattern of Sp1 and Sp3 to the chromosomal DTSS, as well as expression of Sp1 and Sp3 and that Tat directly binds to Sp3 but not Sp1. Furthermore, we observed altered Sp1 and Sp3 levels in the lungs of HIV-1 infected humanized mice.

Methods and Materials

Cell Culture

Wild-type HeLa (ATCC) and HeLa-Tat_{III} cells (NIH AIDS Reagent Program) were grown in OPTI-MEM (Invitrogen Life technologies) supplemented with 3.75% Heat-inactivated fetal bovine serum (Atlanta Biologicals) and 1X Antibiotic/Antimycotic (Invitrogen Life technologies) [16,17]. HeLa-Tat_{III} media also contained 500 μg/mL G418 (Sigma). Primary Human Pulmonary Artery Endothelial cells (HPAEC, from Lonza) were maintained in

EGM2-MV media, (Lonza). All cells were grown in a 37°C incubator containing 6.5% CO_2, washed with 1X phosphate buffered saline (PBS, filter-sterilized) and fed fresh medium every 2–3 days.

In silico identification of putative *sod2* upstream regulator regions

To identify possible novel Sp-regulatory regions upstream of the *sod2* start site, we scanned 3400 nucleotides upstream of the *sod2* promoter, hereafter referred to as −3400sod2, using the openware software packages MatInspector (https://omictools.com/matinspector-tool) and PhysBinder (http://bioit.dmbr.ugent.be/physbinder/index.php). Figure 1 depicts the putative Sp-binding clusters identified.

sod2 promoter-luciferase constructs

Dr. Daret St. Clair generously provided a series of *sod2* promoter-reporter constructs in plasmid pGL3B with luciferase expression under the control of increasingly longer *sod2* upstream sequences (Fig. 1B) [18]. The −210, −1240, −1605, −2987 and −3400 constructs from Dr. St. Clair were used in this study. The −555sod2 construct from St. Clair et al did not fully contain the large Sp-binding cluster that extended out to −584 nucleotides, which we hypothesized would be most strongly regulated by Sp-transcription factors. Thus, we engineered plasmid pGL3B-584sod2 in this study. To generate plasmid pGL3B-584sod2 (SI Table 2), we amplified by polymerase chain reaction (PCR) a 608 bp fragment between −584 and +24 nucleotides with engineered KpnI and BglII restriction sites in the 5' and 3' primers respectively. We used a high fidelity DNA polymerase (AccuPrime, Invitrogen) and included 7-deaza-GTP in the reactions to faithfully amplify across G-C rich sections. After digesting the PCR product and pGL3B parent vector with KpnI-HF and BglII-HF (New England BioLabs) and cleaning up the resulting digests (PCR Clean kit, Qiagen), we ligated the fragment into the vector using standard ligase reaction conditions (Invitrogen) and transformed the ligated product into chemically competent *E. coli* DH5α following the manufacturer's protocol (Stratagene). We selected for Ampicillin-resistant clones by plating on LB-agar plates containing 100 μg/ml of ampicillin and screened by PCR and restriction analysis. Positive clones identified by screening were confirmed by sequencing and we selected a clone with perfect alignment to the endogenous sequence for testing.

Transfections and Dual Luciferase

To measure *sod2* transcription we used promoter-reporter plasmids expressing luciferase under the control of increasingly longer *sod2* upstream sequences (Fig.1) in HPAEC, HeLa WT and HeLa-Tat_{III} cells. Cells were transiently transfected using Superfect transfection reagent according to the manufacturer's protocol (Qiagen). HeLa WT and HeLa-Tat_{III} cells were transfected with 1 μg of total DNA, 0.5 μg of *sod2* promoter-reporter plasmid and 0.5 μg of a CMV driven *Renilla* luciferase plasmid. HPAEC were also co-transfected with 0.5 μg of the Tat-expressing plasmid, pCP2-Tat_{101} (see Supplemental Materials Table 2). Twenty-four hours after transfection, luciferase was measured using the Dual Luciferase Reporter Assay System (Promega,) according to the manufacturer's instructions in a dual injector MicroPlate Luminometer (Promega). All luminescence data was normalized to the *Renilla* signal.

Chromatin Immunoprecipitation

Using Superfect transfection reagent (Qiagen), HPAEC (approximately 2×10^6 cells per dish, six dishes per transfection) were either mock transfected or transfected with 5 μg of pCP2-Tat_{101} plasmid. Twenty-four hours after transfection, cells were cross-linked with 1% formaldehyde and quenched with 1X Glycine followed by two consecutive washes with ice-cold 1X PBS. Cells were collected via scraping in 1X PBS supplemented with protease and phosphatase inhibitors and centrifuged at 3000 × g for 5 minutes. Following the manufacturer's instructions, the Pierce Agarose ChIP Kit (Thermo Scientific) was used to precipitate and clean-up DNA bound by either control IgG (3 μg rabbit or mouse IgG provided in the kit), anti-Sp1 rabbit polyclonal (3 μg, ChIP-grade, Abcam) or Sp3 mouse monoclonal (3 μg, ChIP-grade, Santa Cruz). The purified final DNA was quantified using Qubit® 2.0 Fluorometry (Invitrogen Life Technologies).

ChIP qPCR

A plasmid containing the −3400bp length of *sod2* promoter was used as template for a standard curve ranging from 2×10^8 to 9×10^2 copies (1 ng to 0.5 fg). ChIP qPCR primers flanking the predicted Sp binding sites around the −584 region of *sod2* were designed (Fig.1 and Supplemental Materials Table 1) and the target region was amplified from chromatin DNA that co-immunoprecipitated with anti-Sp1, anti-Sp3 or mouse IgG. qPCR was performed using iQ SYBR Green qPCR Supermix (BioRad) according to manufacturer's instructions. Copy numbers were normalized to ng of DNA.

Gene Transcriptional Analyses

Total RNA was extracted from cells using RNeasy Mini Kit (Qiagen) according to manufacturer spin method protocol. Reactions were carried out as technical duplicates from experimental replicates of each condition. RT-qPCR was carried out with 50 ng of RNA/reaction using iTaq Universal SYBR green one-step RT-qPCR supermix (BioRad). For relative expression analysis, the average Ct values of the technical replicates were analyzed utilizing the delta-delta Ct method, where all samples were normalized to GAPDH (first delta) and then compared to un-treated controls (second delta). Primer sequences are summarized in Supplemental Materials Table 1.

Immunoblots, Immunoprecipitation and DNA-binding ELISAs

Immunoprecipitations were carried out from 1–4 mg of cellular protein with 3 μg of antibody per mg of protein following standard protocols [19]. For immunoblots, total protein was extracted from cells using Mammalian Protein Extraction Reagent (Thermo Fisher) supplemented with 1 mM DTT and 1X Protease/Phosphatase inhibitor cocktail (HALT, Thermo Fisher). For immunoblot analysis, we resolved proteins by Sodium dodecyl sulfate (SDS) poly-acrylamide gel electrophoresis, transferred to Polyvinylidene fluoride (PVDF, BioRad) and detected with antibodies from commercial sources (see Supplemental Materials Table 3). Mouse monoclonal antibody to Tat was from the AIDS Reference Reagent Program [20]. Immunoblots were imaged by chemiluminescence using Supersignal West Femto Maximum Sensitivity substrate (Thermo Fisher) on a Kodak Image Station 440 CF and Kodak 1D imaging software. Background was subtracted from the densitometric net

intensity values of the target protein and the loading control (β-actin), which was used to normalize the signal of the target protein. DNA-binding ELISAs for active Sp1 and Sp3 were carried out on nuclear extracts prepared as previously described [21] using Sp1 and Sp3-specific TransAM kits (Active Motif) according to manufacturer's protocol.

Generation and HIV Infection of Humanized NSG-BLT Mice

Humanized, NSG-BLT, mice were generated at the Humanized Mouse Core of the University of Massachusetts Medical School, as previously described [22]. NOD-scid IL2rg-null mice at 6 to 8 weeks of age were implanted with human fetal thymic and liver tissue (Advanced Bioscience Resources, In., Alameda, CA) and transplanted with autologous human hematopoietic stem cells (hCD34+) derived from the fetal liver. In BLT mice, T cells are autologously educated by the human thymic tissue, and the mice develop a robust human immune system comprised of multiple human cell lineages with sustain high levels of human T cells for several months. At 12 weeks post tissue engraftment, BLT mice were monitored by flow cytometry for human immune system development and human CD45+ cells (clone HI30, BD Bioscience), CD3+ T cells (clone UCHT1, BioLegend) and CD20+ B cells (clone 2H7, BioLegend) were measured. Engrafted BLT mice were shipped to the University of Colorado where they were quarantined for 1 week and then housed in a pathogen-free BSL3-equipped animal laboratory.

Detection of HIV DNA and cell-free RNA in NSG-BLT mice

To validate the HIV infection of NSG-BLT mice, we developed a highly sensitive nested PCR approach targeting the env gene. Two primer pairs (outer and inner reactions) were designed (Supplemental Materials Table 1) and used in PCR with total DNA extracted from homogenized liver tissue (Supplemental Materials Figure 2). We also detected HIV DNA in the same way, with DNA extracted from homogenized lung (Supplemental Materials Figure 2) indicating that infected cells or possibly latently infected cells were present in the lungs at 10 weeks post-infection. Plasmid pBR-NL43-IRES-eGFP-nef+ (AIDS Reference Reagent Program), 3.5 fg, was used as the positive control for this PCR. As negative controls, we included no template reactions and we analyzed, by electrophoresis, the product of the outer reaction to show sensitivity. Further, we quantified cell-free virus in the lungs of infected NSG-BLT by performing bronchoalveolar lavage (BAL) as previously described [15] and collecting the BAL cells by centrifugation at 600×g for 15 minutes at 4°C, which were stored at −80°C. RNA was extracted from the cell-free BAL fluid (supernatant) using QIAamp UltraSens Viral Kit (Qiagen). To generate a template for a standard curve for the HIV RT-qPCR, we amplified a 541 bp fragment of the env gene using the outer primers of the nested PCR (Supplemental Materials Tables 1 and 2) and cloned it into pCR2.1 plasmid via T-A ligation with the TOPO T-A cloning system (Invitrogen Life Technologies) generating plasmid pCR2.1-Env541. We confirmed the clone via sequencing and designed RT-qPCR primers (Supplemental Materials Table 1) within the cloned 541 bp env fragment. We performed RT-qPCR on viral RNA extracted from cell-free BAL fluid using iTaq Universal SYBR green One-step RT-qPCR SYBR supermix (BioRad). From a standard curve generated with plasmid pCR2.1-Env541, we calculated HIV genome copies per ml of BAL fluid (Supplemental Materials Table 4).

Detection of Sp1, Sp3 and SOD2 proteins in lungs of NSG-BLT mice

For detection of Sp1, Sp3 and SOD2 in the lungs of HIV infected NSG-BLT mice, we extracted protein from lung tissue homogenates using Tissue Protein Extraction Reagent (Thermo Fisher) supplemented with 1 mM DTT and 1X Protease/Phosphatase inhibitor cocktail (HALT, Thermo Fisher). For immunoblot analysis, we resolved lung proteins by Sodium dodecyl sulfate (SDS) poly-acrylamide gel electrophoresis, transferred to Polyvinylidene fluoride (PVDF, BioRad) and detected with antibodies from commercial sources (Supplemental Materials Table 3). We used chemiluminescence with Supersignal West Femto Maximum Sensitivity substrate (Thermo Fisher) to detect the proteins on a Kodak Image Station 440 CF and Kodak 1D imaging software to quantify the signals. Background was subtracted from the densitometric net intensity values of the target protein and the loading control (β-actin), which was used to normalize the signal of the target protein.

Measuring Total Antioxidant Capacity in Lungs of NSG-BLT Mice

A chromogenic Antioxidant Assay (Cayman Chemical Co) was used to determine the antioxidant content in total lung homogenates from uninfected, mock-infected and HIV-1 (NL4–3 strain) infected NSG-BLT mice (10 weeks). The assay is based on the ability of antioxidants in the experimental sample to inhibit the oxidation of 2,2'-Azino-di-[3-ethylbenzthiazoline sulphonate] by metmyoglobin. Antioxidant content in the lung homogenates was quantified using a standard curve created with the water-soluble tocopherol analogue Trolox and normalized to mg of lung protein.

Immunohistochemical Detection of SOD2 in NSG-BLT Mouse Lungs

Immunohistochemistry (IHC) was performed to assess SOD2 content in the lungs of humanized NSG-BLT mice that were either uninfected, mock-infected or infected with HIV-1 (NL4–3 strain) for 10 weeks. To euthanize the mice we anesthetized with isoflurane followed by a sub-lethal IP injection (50mg/kg) of ketamine and cervically dislocated after the mice were no longer responsive to tactile stimulus but still had spontaneous respirations. The pulmonary vascular bed was perfused with sterile saline, the left lung lobes were inflated with low-melting agarose to preserve morphology as previously described [15] fixed in formalin, paraffinized and sectioned. Deparaffinization of lung sections was performed using an automated system (Gemini AS, Thermo Scientific) and epitope retrieval was accomplished by boiling deparaffinized lung tissue in a citrate based antigen unmasking solution (Vector Laboratories, pH 6.0) for 30 minutes with a 20 minute cool down. Endogenous peroxidase activity was quenched by incubating in 3% hydrogen peroxide for 10 minutes. SOD2 was detected using a monoclonal antibody (sc-133134 mouse monoclonal IgG_{2b}) with the VECTASTAIN *Elite* ABC Universal Kit and ImmPACT DAB Peroxidase (HRP) Substrate according to manufacturer's instructions (Vector Laboratories). Slides were incubated for 10 seconds in light green counterstain (American Master Tech), cleared using an automated protocol (Gemini AS, Thermo Scientific) and mounted. Images were acquired under bright-field illumination with a Nikon Eclipse E600 microscope.

Results

In silico analysis of potential Sp-mediated regulatory regions upstream of sod2 ORF

Using open sourceware, MatInspector and PhysBinding, we performed *in silico* analysis of DNA sequences up to −3400 bp upstream of the *sod2* transcriptional start and identified clusters of predicted Sp-binding sites. Sp1 and Sp3 are known to most strongly regulate transcription from regions containing clusters of binding sites. Importantly, there was a large Sp-binding cluster predicted between −210 and −584 that we postulated would be likely a bona fide Sp-element since it contained 38 predicted Sp-binding sites (Fig. 1A). Other clusters of potential Sp-binding sites were detected further upstream but these were predicted to have weaker binding affinity and the clusters were smaller, there were fewer potential binding sites than in the −584 clusters.

Tat modulation of sod2 regulatory regions rich in Sp-binding sites

To determine the level of transcription from the potential distal regulatory sites that we identified further upstream of the *sod2* proximal promoter, we transiently transfected a series of sod2promoter-luciferase reporter constructs, shown in Figure 1B, into HeLa cells. We found that expression from the −584sod2-prom construct was stronger (2.3-fold, p=0.0255) than from the proximal −210 region. All other constructs extending further upstream were expressed to the same extent as the −210 construct but none were as strong as −584 (Fig. 2A). This indicated that maximal expression is driven by sequences between −210 and −584 and suggested that sequences upstream of nucleotide −584 may actually repress the maximal expression seen with the −584 construct. Furthermore, the Tat protein repressed transcription of all the constructs, in line with the previous reports that Tat represses *sod2* transcription.

As HeLa cells are known to have numerous pleomorphic defects and chromosomal instabilities related to the transformed phenotype, we investigated the expression of the sod2-prom constructs in human primary cells (HPAEC) in the presence and absence of Tat. As in HeLa cells, in HPAEC maximal expression occurred with the −584sod2-prom construct, which again demonstrated stronger expression than the basal −210 construct (5.1-fold, p<0.0001) (Fig. 2B). Interestingly, in these cells expression of the −1240sod2-prom construct was repressed compare to all other constructs, although expression was restored further upstream with constructs −1605, −2987 and −3406sod2-prom. These observations suggest that the in HPAEC, sequences between −584 and −1240 contain repressive sites but that repression is relieved by sequences upstream of −1240. Expression from all constructs upstream of −1240 is equivalent to −584 and Tat repressed expression from all constructs with the exception of −1240 (not statistically significant). Taken together, these data suggest that the proximal −210 region functions as a minimal promoter but for maximal expression of *sod2*, promoter sequences extend out to nucleotide −584 and that a further repressive motif might be contained between nucleotides −584 and −1240.

Tat modulates the occupancy of Sp1 and Sp3 on sod2 regulatory regions

Our promoter-reporter data point to the −584 construct as containing the maximal *sod2* promoter, the activity of which is, all but eliminated, by Tat in HPAEC. As Sp1 and Sp3 are the transcription factors principally responsible for basal *sod2* transcription, we

hypothesized that Sp-binding on the large cluster of Sp-binding sites located on the −584sod2-prom construct is required for maximal *sod2* transcription and that the HIV-Tat protein modulates Sp-transactivation at the −584 region of this promoter. To test this hypothesis, we used chromatin immunoprecipitation (ChIP) to determine the occupancy levels of Sp1 and Sp3 on the Sp clusters at the −584 region of the endogenous *sod2* promoter in Tat-transfected HPAEC. Figure 3 demonstrates that Tat expression in HPAEC resulted in a dramatic increase in the ratio of Sp1 to Sp3 bound to the −584 region of the endogenous *sod2* promoter (775-fold increase in ratio). This effect appears to be due to both an increase in the amount of bound Sp1 as well as a concurrent decrease in bound Sp3, suggesting a predilection for Sp1 complexes to outcompete Sp3 for occupancy of the endogenous *sod2* promoter in the presence of Tat.

Tat stimulates expression of endogenous sod2 in HPAEC

As the ChIP results indicated that Tat alters the binding of Sp1 and Sp3 on a cis-element of the endogenous *sod2* promoter that is rich in Sp-binding sites, we next sought to determine if Tat alters the transcription of endogenous *sod2* in HPAEC. RT-qPCR showed that Tat strongly stimulates (~20-fold) transcription of *sod2* in HPAEC (Fig. 4A). Furthermore, immunoblot analysis showed that Tat also resulted in increased SOD2 protein levels (Figs. 4B and 4C). These findings are in agreement with previous observations that higher Sp1 to Sp3 ratios results in increased SOD2 expression.

Tat alters total cellular Sp3 activity but not Sp1 activity

It has been demonstrated that the Sp1 to Sp3 ratio is an important regulator of SOD2 expression, and that Sp1 acts to stimulate expression through interaction with the *sod2* promoter. Given that Tat stimulated endogenous expression of SOD2, possibly by altering the relative binding of Sp1 and Sp3 to the *sod2* promoter, we next sought to address if the changes in Sp1 and Sp3 binding to −584sod2-prom might result from changes in total cellular Sp1 and Sp3 DNA binding activity. Utilizing nuclear protein extracts from un-transfected and Tat-transfected HPAEC, we performed a DNA-binding ELISA. While Tat had no effect on the total cellular levels of active Sp1, the amount of active Sp3 was reduced some 20% in the presence of Tat (Fig. 5). These results demonstrate that Tat likely acts to modulate the Sp1 to Sp3 binding ratio through inhibition of Sp3 and not via enhancement of Sp1.

Tat Co-immunoprecipitates with Sp3 but not Sp1 and does not affect the acetylation state of Sp3

HPAEC were transfected with a Tat-expressing vector and co-immunoprecipitation assays performed on total cellular lysates. While Tat never appeared as a co-immunoprecipitate with Sp1 (Supplemental Materials Fig.1), it did immunoprecipitate with Sp3 (Fig.6). Numerous studies have reported that acetylation of Sp3 influences binding and transcriptional activity. Additionally, other studies show that Tat alters cellular acetylates and deacetylases and the cellular pathways that they control. In order to observe the effects of Tat on acetylation of Sp3, endogenous Sp3 was immunoprecipitated from un-transfected or Tat transfected HPAEC, and the acetylation state probed via immunoblot with a pan-acetyl lysine antibody. Figure 6B demonstrates that the acetylation state of Sp3 remains unchanged

in the presence of Tat, which suggests that Tat may be impeding the ability of Sp3 to compete with Sp1 for the *sod2* promoter by physical or steric inhibition but not by altering its acetylation.

Tat alters expression of Sp1 and Sp3

Lastly, we surmised that Tat could also be altering the binding and activity of Sp1 and Sp3 on the endogenous *sod2* promoter by affecting cellular levels of either protein. To investigate this, we quantified Sp1 and Sp3 transcript and protein levels in the presence and absence of Tat. Interestingly, Tat stimulated transcription of Sp3 by more than 4.5 fold but transcription of Sp1 was only changed 2-fold (Fig.7), such that the relative amounts of Sp3 and Sp1 transcription in the cells were significantly changed. Furthermore, immunoblot analysis confirmed that Tat changed Sp1 and Sp3 protein levels in a manner similar to the transcript levels. (Fig.8).

HIV-1 infection alters Sp3 and SOD2 expression in the lungs of infected humanized NSG-BLT mice

Given the effects of Tat on Sp1/Sp3 and SOD2 in HPAEC, we surmised that a similar effect might be observed in the context of HIV-1 infection. Many oxidative stress related inflammatory comorbidities manifest in the lungs of HIV patients, and we had previously demonstrated increased SOD2 expression as well as biomarkers of oxidative stress in the lungs of an HIV Tat-transgenic mouse model. In this study, we harvested whole lung tissue from HIV-1 infected humanized NSG-BLT mice for analysis. We thoroughly validated HIV infection of these mice by detecting HIV DNA in the liver and lungs (Supplemental Materials Figure 2) and we confirmed the presence of viral replication in the lungs by detecting cell-free viral RNA (Supplemental Materials Table 4) in bronchoalveolar lavage fluid (BALf). Immunoblotting assays demonstrated no detectable difference in Sp1 levels between mock infected and HIV infected mice. However, in agreement with our observations in HPAEC, Sp3 levels were increased ~2-fold in lung tissue from HIV infected mice compared to vehicle control, but Sp1 levels were not significantly changed (Fig. 10). SOD2 levels did not appear to significantly altered in the total lung homogenates of HIV infected mice as analyzed by western blot (fig. 8). We surmised that SOD2 upregulation may be localized, for example in cells/tissues that would be in close proximity to circulating Tat and/or HIV infected cells, and thus the effect was diluted out when whole lung tissue was processed. In order to more precisely observe SOD2 levels in the lungs as well as to observe the potential tissue-specific sites of SOD2 regulation, we performed IHC on lung tissue cross sections of HIV infected and uninfected humanized NSG-BLT mice. Staining for SOD2 revealed increased periadventitial expression (Fig. 11A and Supplemental Materials Fig.5).

Total antioxidant capacity is decreased in the lungs of HIV infected humanized NSG-BLT mice

The observation that SOD2 is upregulated in the lungs of infected mice is in agreement with previous findings that Sod2 is upregulated in the lungs of a Tat transgenic mouse model in which Tat expression is specific for the alveolar space. Despite this effect, all evidence points to increased oxidative burden in these animals nevertheless. SOD2 is only one

component in a large and intricate system of redox balancing proteins, and while SOD2 levels may be increased, the overall net oxidative burden may still be greater than basal levels should other anti-oxidant systems be affected. As such, we measured the total antioxidant capacity (TAC) of total lung tissue extract from HIV infected and uninfected humanized NSG-BLT mice. In line with previous observations, TAC is lower in the lungs of HIV infected mice (Fig. 11B).

Discussion

Modern antiretroviral therapy has proven successful in the management of HIV infection by controlling viral load and preventing the progression of the disease to the AIDS phenotype. Nonetheless, patients remain chronically infected as HIV resides in active and latent reservoirs. This is evidenced by the detection of proviral DNA as well as genomic RNA and soluble viral factors in a variety of tissues including the lungs, liver, lymph nodes, and gastrointestinal tract [23–25]. The ability to control HIV infection but the inability to completely clear the virus from infected individuals renders infection with HIV a chronic condition that carries with it the risk of developing a variety of HIV associated co-morbidities including pulmonary arterial hypertension, COPD, HIV associated dementia, and inflammatory liver disease [26–28]. While the mechanisms driving these HIV-associated pathologies are complex and heterogeneous, persistent oxidative stress and inflammation are shared conditions which are heavily implicated as contributing factors to disease progression. A number of soluble HIV factors have been demonstrated to elicit oxidative stress including Gp120, Nef, Vpr and Tat [29–31]. However, Tat represents a target of particular interest due to the fact that it is secreted in large amounts from infected cells into circulation where it is internalized by uninfected bystander cells. This characteristic of Tat has been long established, and recent research demonstrates that Tat secretion may be even more prolific than previously anticipated. Rayne et. al. have demonstrated that nuclear accumulation of Tat is not required for efficient and successful transactivation of the viral LTR, and in fact the majority of Tat localizes to the plasma membrane of primary T-cells and approximately two thirds of Tat produced is secreted into the extracellular environment [32,33]. Congruently, Tat has been detected in the serum of HIV infected patients receiving anti-retroviral therapy at concentrations as high as 9.02 ng/mL [34]. We chose to observe the effects of Tat in primary human pulmonary arterial endothelial cells (HPAEC) due to the heavy involvement of the endothelium in deadly HIV associated lung co-morbidities such as pulmonary arterial hypertension. Additionally, the endothelium is likely exposed to a large amount of Tat in HIV infected patients either through contact with secreted extracellular Tat and/or intimate contact with infected T-cells and Monocytes.

HIV appropriates and manipulates a plethora of cellular transcriptional and post translational factors in order to augment its own life cycle. One of the most well characterized transcriptional complexes that HIV utilizes is NF-κB. The HIV LTR contains two adjacent NF-κB binding sites, and induction of NF-κB activity greatly enhances viral replication [35,36]. As such, the pro-oxidant environment induced by HIV may represent a mechanism through which HIV induces inflammation and activation of inflammatory transcriptional elements, which enhance viral transcription. Repression of SOD2 by Tat provided an early clue as to one mechanism by which HIV may induce a pro-oxidant environment, and it was

subsequently demonstrated that the viral manipulation of SOD2 was achieved through modulation of Sp1/Sp3 activity by Tat [14]. Sp1 and Sp3 are highly homologous transcription factors with conserved DNA binding domains which often compete to occupy the same nucleotide sequences. Interestingly, Sp1 activity has been demonstrated to enhance viral replication via synergism with NF-κB as well as by facilitating viral particle assembly [37,38]. Conversely, Sp3 has been demonstrated to have a repressive effect on the HIV LTR [39], demonstrating the dichotomous activity of these two highly similar transcription factors. While these studies provided insight into the mechanisms by which SOD2 may be effected by Tat, the Tat mediated interactions of Sp1 and Sp3 were only studied in the proximal *sod2* promoter (−210 nt) and relied on transformed cell lines as well as Sp factor deficient *Drosophila* S2 cells. We have hypothesized that additional Sp binding sites in more distal regions of the *sod2* promoter may also be affected by Tat and that expression of SOD2 would be consequently altered. Here, we identified a particularly Tat sensitive region in a more distal location (−584 nt, DTSS) of the *sod2* promoter and demonstrated that this sensitivity is a result of Tat mediated alteration of Sp1 and Sp3 binding, resulting in increased expression of SOD2 in HPAEC. Additionally, we observed a similar increase in levels of Sp3 in whole lung tissue from HIV-1 infected humanized mice.

In silico analysis revealed a large number of putative Sp binding sites in the distal *sod2* promoter out to −3406 nts from the proximal Tat sensitive site. As such, we utilized a series of increasingly long *sod2* promoter driven luciferase constructs to observe levels of *sod2* promoter activity in constitutively Tat expressing HeLa cells (HeLa-Tat_{III}) as well as in mock transfected (Tat(−)) or Tat transfected (Tat(+)) HPAEC. In the absence of Tat, reporter expression was highest from the −584sod2-pGL3B construct. In each case, the expression from −584sod2-pGL3B was significantly higher than from the proximal −210sod2-pGL3B vector (2.3 fold greater in HeLa, and 5.1 fold greater in HPAEC). In Tat_{III} cells, expression was repressed in every instance with the exception of −1605sod2-pGL3B (not statistically significant). When HPAEC were co-transfected with the sod2 promoter vectors and a Tat-expressing vector, expression was repressed in every instance with the exception of −1240sod2-pGL3B, suggesting that there were indeed Tat sensitive Sp (TSS) binding elements in the distal regions of the *sod2* promoter. ChIP analysis of the −584 *sod2* promoter region in HPAEC subsequently revealed a dramatic shift in Sp1/Sp3 occupancy from an approximately equivalent level in Tat(−) cells to a ~1000:1 Sp1 to Sp3 ratio in Tat(+) cells. This observation is surprising as high Sp1 to Sp3 ratios generally result in transcriptional activation of promoters containing Sp sites, although we observed repression of *sod2*promoter activity in the presence of Tat from our reporter constructs. In agreement with our ChIP analysis, SOD2 transcription as well as expression was enhanced by Tat in HPAEC, suggesting that the presence of Tat indeed alters Sp binding activity in a manner that facilitates SOD2 transcription. The dichotomy between the reporter construct results and cellular SOD2 levels in Tat(+) HPAEC may be explained by the fact that a powerful intronic *sod2* enhancer is absent in the reporters as the *sod2* ORF is replaced by the luciferase gene. Sp1 acts to facilitate *sod2* transcription by acting to bridge the promoter to the *sod2* intronic enhancer through an 11G loop in the proximal promoter [40]. In the absence of this enhancer, no such interaction can occur, and Tat mediated Sp1 accumulation to *sod2* promoters on plasmids may in fact result in reduced reporter expression.

In an effort to elucidate potential mechanisms by which Tat may alter Sp1/Sp3 binding affinity, we performed competitive DNA-binding ELISA with nuclear protein extracts from Tat(+) and Tat(−) HPAEC. Tat had no effect on Sp1 binding activity, while Sp3 binding activity was significantly reduced, suggesting that Tat does not enhance Sp1 binding, but rather reduces Sp3 binding, allowing Sp1 to outcompete Sp3 for occupancy of the *sod2* promoter Tat is itself a transcription factor and is known to form complexes with a number of cellular transcriptional regulators including Lysine Acetyl Transferase 5 (Kat5) and P300/CBP-associated factor (PCAF). Tat represses the activity of Kat5 [41] but enhances that of PCAF [42], demonstrating that Tat has pleiotropic effects on different transcriptional elements. As such, we found it reasonable to hypothesize that Tat may complex or otherwise interact directly with either Sp1 and/or Sp3 in order to elicit the effects observed in HPAEC. Endogenous Sp3 co-immunoprecipitated with Tat in HPAEC, while Sp1 did not, indicating that Tat may alter Sp3 binding activity through direct interaction and physical or steric inhibition. While Tat led to increased levels of Sp1 transcript (~2-fold increase), Sp3 transcription was even more highly upregulated by Tat (~4.5 fold), further strengthening the hypothesis that Tat interferes with Sp3 activity through inhibition of binding to the promoter rather than by repressing expression. Immunoblot confirmed the RT-qPCR results, as the ratios of Sp3 to Sp1 protein reflected the ratios of Sp1 to Sp3 transcript in Tat(+) HPAEC. The increase in Sp3 expression may in fact be a compensatory response by the cells, as Tat results in global repression of Sp3 activity, cells may attempt to restore this through upregulation of the gene. Sp1 and Sp3 are also known to be induced by oxidative stress [43], and the pro-oxidant environment elicited by Tat may also be driving their enhanced expression. Finally, we speculated that Sp1 and Sp3 levels as well as SOD2 levels would be altered in lungs in the context of HIV infection. To this end, we collected and probed whole lung tissue from uninfected, mock infected, or HIV-1 infected humanized mice for analysis. Immunoblot analysis demonstrated a significant increase in Sp3 levels, while no significant increase in Sp1 or SOD2 was observed. The fact that SOD2 appeared unaffected in HIV infected mice was surprising, and we surmised that tissues most proximal to circulating Tat and HIV infected cells (such as the pulmonary endothelium and lung vascular tunica media) would be most likely to be effected and that this was perhaps undetectable from whole tissue extract by western blot. As such, we performed immunohistochemistry on lung sections from HIV infected and uninfected mice. Indeed, we observed an increase in SOD2 expression in periadventitial structures. Previous studies have demonstrated that, while SOD2 levels are increased in Tat transgenic animals, oxidative burden is still higher. To this end, we measured the total antioxidant capacity of whole lung tissue from HIV infected and uninfected mice. In agreement with previous observations, the total antioxidant capacity was lower, suggesting that SOD2 upregulation in the context of HIV infection is insufficient to restore the lung redox balance.

Redox imbalance is a critical factor in the HIV life cycle and well established consequence of HIV infection and oxidative stress is a unifying factor across a vast array of HIV associated co-morbidities. In previous studies, Tat has been demonstrated to have a repressive effect on SOD2 expression by proxy of altering Sp1/Sp3 binding to the proximal *sod2* promoter [44], though the reliance on artificial promoter constructs as well as transformed cell lines has left an incomplete picture of how Tat may interact with these

transcription factors and effect SOD2 in more physiologically relevant systems. Here, we have observed that Tat indeed alters Sp1/Sp3 activity and as such, modulates endogenous SOD2 expression in primary HPAEC. However, our observations suggest that, in these cells, Tat represses the binding activity Sp3 and allows Sp1 to more effectively occupy not only the proximal but the distal regions of the *sod2* promoter as well. Furthermore, we demonstrated that HIV infection in humanized mice results in upregulation of Sp3 in the lungs and localized increase of SOD2. Taken together, these observations support the hypothesis that Tat dysregulates the Sp1/Sp3 transcriptional network by directly altering the properties of these transcription factors, which may have deleterious impacts on global transcriptional regulation in response to oxidative stress.

Supplementary Material

Refer to Web version on PubMed Central for supplementary material.

Acknowledgements

This work was supported by the National Institutes of Health grant R01HL125050. The following reagent was obtained through the NIH AIDS Reagent Program, Division of AIDS, NIAID, NIH: HeLa-tat-III Cells (cat# 502) from Drs. William Haseltine, Ernest Terwilliger and Joseph Sodroski. The following reagent was obtained through the NIH AIDS Reagent Program, Division of AIDS, NIAID, NIH: Anti-HIV-1 HXB2 Tat Monoclonal antibody (cat# 7377) from Dr. Dag E. Helland. The following reagent was obtained through the NIH AIDS Reagent Program, Division of AIDS, NIAID, NIH: pBR-NL43-IRES-eGFP-nef+ plasmid (cat#11371) from Dr. Frank Kirchhoff.

Funding: This work was funded by the National Institutes of Health grant number R01HL125050

Literature Cited

[1]. Triplette M, Crothers K, Attia EF, Non-infectious Pulmonary Diseases and HIV, Curr. HIV/AIDS Rep 13 (2016) 140–148. doi:10.1007/s11904-016-0313-0. [PubMed: 27121734]

[2]. Ivanov AV, Valuev-Elliston VT, Ivanova ON, Kochetkov SN, Starodubova ES, Bartosch B, Isaguliants MG, Oxidative Stress during HIV Infection: Mechanisms and Consequences, Oxid. Med. Cell. Longev 2016 (2016) 1–18. doi:10.1155/2016/8910396.

[3]. Flores SC, Marecki JC, Harper KP, Bose SK, Nelson SK, McCord JM, Tat protein of human immunodeficiency virus type 1 represses expression of manganese superoxide dismutase in HeLa cells., Proc. Natl. Acad. Sci. U. S. A 90 (1993) 7632–7636. [PubMed: 8395050]

[4]. Marciniak RA, Calnan BJ, Frankel AD, Sharp PA, HIV-1 Tat Protein Tram-Activates Transcription In Vitro, Cell. 63 (1990) 791–602. http://ac.els-cdn.com.hsl-ezproxy.ucdenver.edu/0092867490901455/1-s2.0-0092867490901455-main.pdf?_tid=6981dc22-29f9-11e7-ab10-00000aacb362&acdnat=1493153865_fe00eca4a54c090b8ebd8f06c10a95cf (accessed April 25, 2017). [PubMed: 2225077]

[5]. Marciniak RA, Sharp PA, HIV-1 Tat protein promotes formation of more-processive elongation complexes, EMBO J. 1013 (1991) 4189–4196. https://www.ncbi.nlm.nih.gov/pmc/articles/PMC453171/pdf/emboj00111-0201.pdf (accessed April 25, 2017).

[6]. Chang HC, Samaniego F, Nair BC, Buonaguro L, Ensoli B, HIV-1 Tat protein exits from cells via a leaderless secretory pathway and binds to extracellular matrix-associated heparan sulfate proteoglycans through its basic region, (1997).

[7]. Col E, Caron C, Chable-Bessia C, Legube G, Gazzeri S, Komatsu Y, Yoshida M, Benkirane M, Trouche D, Khochbin S, HIV-1 Tat targets Tip60 to impair the apoptotic cell response to genotoxic stresses., EMBO J. 24 (2005) 2634–45. doi:10.1038/sj.emboj.7600734. [PubMed: 16001085]

[8]. Ma S, Fu A, Chiew GGY, Luo KQ, Hemodynamic shear stress stimulates migration and extravasation of tumor cells by elevating cellular oxidative level., Cancer Lett. 388 (2017) 239–248. doi:10.1016/j.canlet.2016.12.001. [PubMed: 27965040]

[9]. Pauwels RA, Rabe KF, Burden and clinical features of chronic obstructive pulmonary disease (COPD)., Lancet (London, England). 364 (n.d.) 613–20. doi:10.1016/S0140-6736(04)16855-4.

[10]. Pocernich CB, Sultana R, Mohmmad-Abdul H, Nath A, Butterfield DA, HIV-dementia, Tat-induced oxidative stress, and antioxidant therapeutic considerations, Brain Res. Rev 50 (2005) 14–26. doi:10.1016/j.brainresrev.2005.04.002. [PubMed: 15890409]

[11]. Copin JC, Gasche Y, Chan PH, Overexpression of copper/zinc superoxide dismutase does not prevent neonatal lethality in mutant mice that lack manganese superoxide dismutase, Free Radic. Biol. Med 28 (2000) 1571–1576. doi:10.1016/S0891-5849(00)00280-X. [PubMed: 10927183]

[12]. Hernandez-Saavedra D, Swain K, Tuder R, V Petersen S, Nozik-Grayck E, Redox Regulation of the Superoxide Dismutases SOD3 and SOD2 in the Pulmonary Circulation., Adv. Exp. Med. Biol 967 (2017) 57–70. doi:10.1007/978-3-319-63245-2_5. [PubMed: 29047081]

[13]. Xu Y, Porntadavity S, St Clair DK, Transcriptional regulation of the human manganese superoxide dismutase gene: the role of specificity protein 1 (Sp1) and activating protein-2 (AP-2)., Biochem. J 362 (2002) 401–12. doi:10.1042/0264-6021:3620401. [PubMed: 11853549]

[14]. Marecki JC, Cota-Gomez A, Vaitaitis GM, Honda JR, Porntadavity S, St Clair DK, Flores SC, HIV-1 Tat regulates the SOD2 basal promoter by altering Sp1/Sp3 binding activity., Free Radic. Biol. Med 37 (2004) 869–80. doi:10.1016/j.freeradbiomed.2004.06.016. [PubMed: 15706661]

[15]. Cota-Gomez A, Flores AC, Ling XF, Varella-Garcia M, Flores SC, HIV-1 Tat increases oxidant burden in the lungs of transgenic mice, Free Radic. Biol. Med. 51 (2011) 1697–1707. doi:10.1016/j.freeradbiomed.2011.07.023. [PubMed: 21855628]

[16]. Rosen CA, Sodroski JG, Campbell K, Haseltine WA, Construction of recombinant murine retroviruses that express the human T-cell leukemia virus type II and human T-cell lymphotropic virus type III trans activator genes., J. Virol 57 (1986) 379–84. http://www.ncbi.nlm.nih.gov/pubmed/3001360 (accessed September 27, 2019). [PubMed: 3001360]

[17]. Terwilliger E, Proulx J, Sodroski J, Haseltine WA, Cell lines that express stably env gene products from three strains of HIV-1., J. Acquir. Immune Defic. Syndr 1 (1988) 317–23. http://www.ncbi.nlm.nih.gov/pubmed/3265154 (accessed September 27, 2019). [PubMed: 3265154]

[18]. Xu Y, Kiningham KK, Devalaraja MN, Yeh CC, Majima H, Kasarskis EJ, St Clair DK, An intronic NF-kappaB element is essential for induction of the human manganese superoxide dismutase gene by tumor necrosis factor-alpha and interleukin-1beta., DNA Cell Biol. 18 (1999) 709–22. doi:10.1089/104454999314999. [PubMed: 10492402]

[19]. Bonifacino JS, Gershlick DC, Dell'Angelica EC, Immunoprecipitation, in: Curr. Protoc. Cell Biol, John Wiley & Sons, Inc., Hoboken, NJ, USA, 2016. doi:10.1002/cpcb.3.

[20]. Valvatne H, Szilvay AM, Helland DE, A monoclonal antibody defines a novel HIV type 1 Tat domain involved in trans-cellular trans-activation., AIDS Res. Hum. Retroviruses. 12 (1996) 611–9. doi:10.1089/aid.1996.12.611. [PubMed: 8743086]

[21]. Cota-Gomez A, Flores NC, Cruz C, Casullo A, Aw TY, Ichikawa H, Schaack J, Scheinman R, Flores SC, The Human Immunodeficiency Virus-1 Tat Protein Activates Human Umbilical Vein Endothelial Cell E-selectin Expression via an NF-κB-dependent Mechanism, J. Biol. Chem. 277 (2002) 14390–14399. doi:10.1074/jbc.M108591200. [PubMed: 11827962]

[22]. Aryee KE, Shultz LD, Brehm MA, Immunodeficient mouse model for human hematopoietic stem cell engraftment and immune system development, Methods Mol. Biol. 1185 (2014) 267–278. doi:10.1007/978-1-4939-1133-2_18. [PubMed: 25062635]

[23]. Henrich TJ, Hatano H, Bacon O, Hogan LE, Rutishauser R, Hill A, Kearney MF, Anderson EM, Buchbinder SP, Cohen SE, Abdel-Mohsen M, Pohlmeyer CW, Fromentin R, Hoh R, Liu AY, McCune JM, Spindler J, Metcalf-Pate K, Hobbs KS, Thanh C, Gibson EA, Kuritzkes DR, Siliciano RF, Price RW, Richman DD, Chomont N, Siliciano JD, Mellors JW, Yukl SA, Blankson JN, Liegler T, Deeks SG, HIV-1 persistence following extre277277mely early initiation of antiretroviral therapy (ART) during acute HIV-1 infection: An observational study, PLoS Med. 14 (2017). doi:10.1371/journal.pmed.1002417.

[24]. Kuo H-H, Lichterfeld M, Recent progress in understanding HIV reservoirs., Curr. Opin. HIV AIDS 13 (2018) 137–142. doi:10.1097/COH.0000000000000441. [PubMed: 29232209]

[25]. Costiniuk CT, Jenabian M-A, The lungs as anatomical reservoirs of HIV infection., Rev. Med. Virol 24 (2014) 35–54. doi:10.1002/rmv.1772. [PubMed: 24151040]

[26]. Chi D, Henry J, Kelley J, Thorpe R, Smith JK, Krishnaswamy G, Quezada M, Martin-Carbonero L, Soriano V, Vispo E, Valencia E, Moreno V, De Isla LP, Lennie V, Almería C, Zamorano JL, Manuscript A, Structures T, Lund AK, Lucero J, Herbert L, Liu Y, Naik JS, Almodovar S, Jarrett H, Barnett C, Mehta NJ, Khan IA, Mehta RN, Sepkowitz DA, Warburg O, Sitbon O, Lascoux-Combe C, Delfraissy JF, Yeni PG, Raffi F, De Zuttere D, Gressin V, Clerson P, Sereni D, Simonneau G, Rai PR, Cool CD, King JAC, Stevens T, Burns N, Winn RA, Kasper M, Voelkel NF, Shiels MS, Pfeiffer RM, Gail MH, Hall HI, Li J, Chaturvedi AK, Bhatia K, Uldrick TS, Yarchoan R, Goedert JJ, Engels EA, Almodovar S, Cicalini S, Petrosillo N, Flores SC, Prevalence of HIV-related pulmonary arterial hypertension in the current antiretroviral therapy era, Chest. 118 (2011) 108–113. doi:10.1378/chest.09-3065.

[27]. Lorenc A, Ananthavarathan P, Lorigan J, Jowata M, Brook G, Banarsee R, The prevalence of comorbidities among people living with HIV in Brent: a diverse London Borough., London J. Prim. Care (Abingdon) 6 (2014) 84–90. doi:10.1080/17571472.2014.11493422.

[28]. Gingo MR, Morris A, Pathogenesis of HIV and the lung, Curr. HIV/AIDS Rep. 10 (2013) 42–50. doi:10.1007/s11904-012-0140-x. [PubMed: 23079728]

[29]. Staitieh BS, Ding L, Neveu WA, Spearman P, Guidot DM, Fan X, HIV-1 decreases Nrf2/ARE activity and phagocytic function in alveolar macrophages, J. Leukoc. Biol 102 (2017) 517–525. doi:10.1189/jlb.4A0616-282RR. [PubMed: 28550120]

[30]. Sami Saribas A, Cicalese S, Ahooyi TM, Khalili K, Amini S, Sariyer IK, HIV-1 Nef is released in extracellular vesicles derived from astrocytes: evidence for Nef-mediated neurotoxicity., Cell Death Dis. 8 (2017) e2542. doi:10.1038/cddis.2016.467. [PubMed: 28079886]

[31]. Simenauer A, Assefa B, Rios-Ochoa J, Geraci K, Hybertson B, Gao B, McCord J, Elajaili H, Nozik-Grayck E, Cota-Gomez A, Repression of Nrf2/ARE regulated antioxidant genes and dysregulation of the cellular redox environment by the HIV Transactivator of Transcription, Free Radic. Biol. Med 141 (2019) 244–252. doi:10.1016/j.freeradbiomed.2019.06.015. [PubMed: 31238128]

[32]. Rayne F, Debaisieux S, Yezid H, Lin YL, Mettling C, Konate K, Chazal N, Arold ST, Pugnière M, Sanchez F, Bonhoure A, Briant L, Loret E, Roy C, Beaumelle B, Phosphatidylinositol-(4,5)-bisphosphate enables efficient secretion of HIV-1 Tat by infected T-cells, EMBO J. 29 (2010) 1348–1362. doi:10.1038/emboj.2010.32. [PubMed: 20224549]

[33]. Rayne F, Debaisieux S, Bonhoure A, Beaumelle B, HIV-1 Tat is unconventionally secreted through the plasma membrane, Cell Biol. Int. 34 (2010) 409–413. doi:10.1042/CBI20090376. [PubMed: 19995346]

[34]. El-Amine R, Germini D, V Zakharova V, Tsfasman T, V Sheval E, Louzada RAN, Dupuy C, Bilhou-Nabera C, Hamade A, Najjar F, Oksenhendler E, Lipinski M, V Chernyak B, Vassetzky YS, HIV-1 Tat protein induces DNA damage in human peripheral blood B-lymphocytes via mitochondrial ROS production., Redox Biol. 15 (2018) 97–108. doi:10.1016/j.redox.2017.11.024. [PubMed: 29220699]

[35]. Hiscott J, Kwon H, Génin P, Hostile takeovers: Viral appropriation of the NF-κB pathway, J. Clin. Invest 107 (2001) 143–151. doi:10.1172/JCI11918. [PubMed: 11160127]

[36]. Stroud JC, Oltman A, Han A, Bates DL, Chen L, Structural basis of HIV-1 activation by NF-kappaB--a higher-order complex of p50:RelA bound to the HIV-1 LTR., J. Mol. Biol 393 (2009) 98–112. doi:10.1016/j.jmb.2009.08.023. [PubMed: 19683540]

[37]. Datta SAK, Clark PK, Fan L, Ma B, Harvin DP, Sowder RC, Nussinov R, Wang Y-X, Rein A, Dimerization of the SP1 Region of HIV-1 Gag Induces a Helical Conformation and Association into Helical Bundles: Implications for Particle Assembly, J. Virol 90 (2016) 1773–1787. doi:10.1128/jvi.02061-15. [PubMed: 26637452]

[38]. Parrott C, Seidner T, Duh E, Leonard J, Theodore TS, Buckler-White A, Martin MA, Rabson AB, Variable role of the long terminal repeat Sp1-binding sites in human immunodeficiency virus replication in T lymphocytes., J. Virol 65 (1991) 1414–9. http://www.ncbi.nlm.nih.gov/pubmed/1995951 (accessed September 28, 2019). [PubMed: 1995951]

[39]. Majello B, De Luca P, Hagen G, Suske G, Lania L, Different members of the Sp1 multigene family exert opposite transcritional regulation of the long terminal repeat of HIV-1, Nucleic Acids Res. 22 (1994) 4914–4921. doi:10.1093/nar/22.23.4914. [PubMed: 7800480]

[40]. Xu Y, Fang F, Dhar SK, St. Clair WH, Kasarskis EJ, St. Clair DK, The role of a single-stranded nucleotide loop in transcriptional regulation of the human sod2 gene, J. Biol. Chem 282 (2007) 15981–15994. doi:10.1074/jbc.M608979200. [PubMed: 17426024]

[41]. Creaven Martina, Hans Fabienne, Mutskov Vesco, Col Edwige, Caron Cécile, and Dimitrov Stefan, Saadi Khochbin, Control of the Histone-Acetyltransferase Activity of Tip60 by the HIV-1 Transactivator Protein, Tat, (1999). doi:10.1021/BI9907274.

[42]. Quy VC, Pantano S, Rossetti G, Giacca M, Carloni P, HIV-1 Tat binding to PCAF bromodomain: Structural determinants from computational methods, Biology (Basel). 1 (2012) 277–296. doi:10.3390/biology1020277. [PubMed: 24832227]

[43]. Ryu H, Lee J, Zaman K, Kubilis J, Ferrante RJ, Ross BD, Neve R, Ratan RR, Sp1 and Sp3 are oxidative stress-inducible, antideath transcription factors in cortical neurons., J. Neurosci 23 (2003) 3597–606. http://www.ncbi.nlm.nih.gov/pubmed/12736330 (accessed September 28, 2019). [PubMed: 12736330]

[44]. Porntadavity S, Nath A, Prachayasittikul V, Cota-Gomez A, Flores SC, St Clair DK, Different roles of Sp family members in HIV-1 Tat-mediated manganese superoxide dismutase suppression in hepatocellular carcinoma cells., DNA Cell Biol. 24 (2005) 299–310. doi:10.1089/dna.2005.24.299. [PubMed: 15869407]

Highlights

In Human Pulmonary Artery Endothelial Cells (HPAEC), the HIV-Tat Protein:

- Stimulates expression of endogenous sod2
- Modulates sod2 regulatory regions rich in Sp-binding sites
- Alters expression of Sp1 and Sp3
- Alters total cellular Sp3 but not Sp1 DNA binding activity
- Co-immunoprecipitates with Sp3 but not Sp1
- Does not affect the acetylation of Sp3

In humanized NSG-BLT Mice, HIV infection:

- Stimulates expression of total pulmonary Sp3 but not Sp1
- Increases SOD2 expression in the lung periadventitial structures

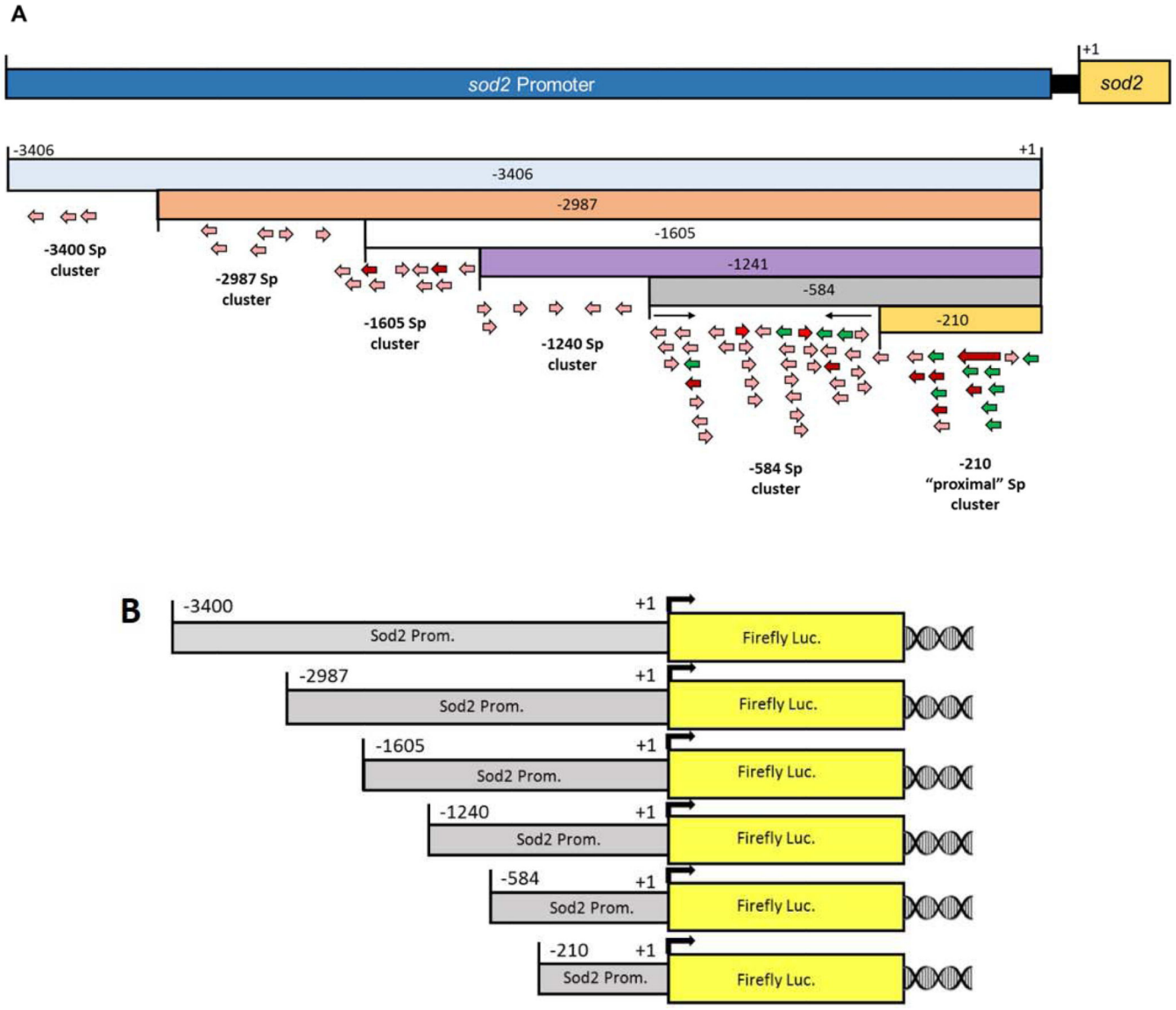

Figure 1. Schematics of predicted Sp binding clusters and Sod2 promoter constructs.

A) Sp-binding clusters in sequences upstream of the sod2 transcriptional start site as predicted by MatInspector and PhysBinder algorithmns: MatInspector predictions = pink/red, PhysBinder = green. Darker shades signify stronger predicted Sp binding affinity. Black arrows indicate locations of ChIP qPCR primers. *B) Sod2-promoter-reporter constructs (sod2-prom) utilized in this study:* Constructs of −210, −1240, −1605, −2987 and −3406 sod2-prom plasmids were a kind gift from Dr. Daret St. Clair. Construct of −584 sod2prom was created in house.

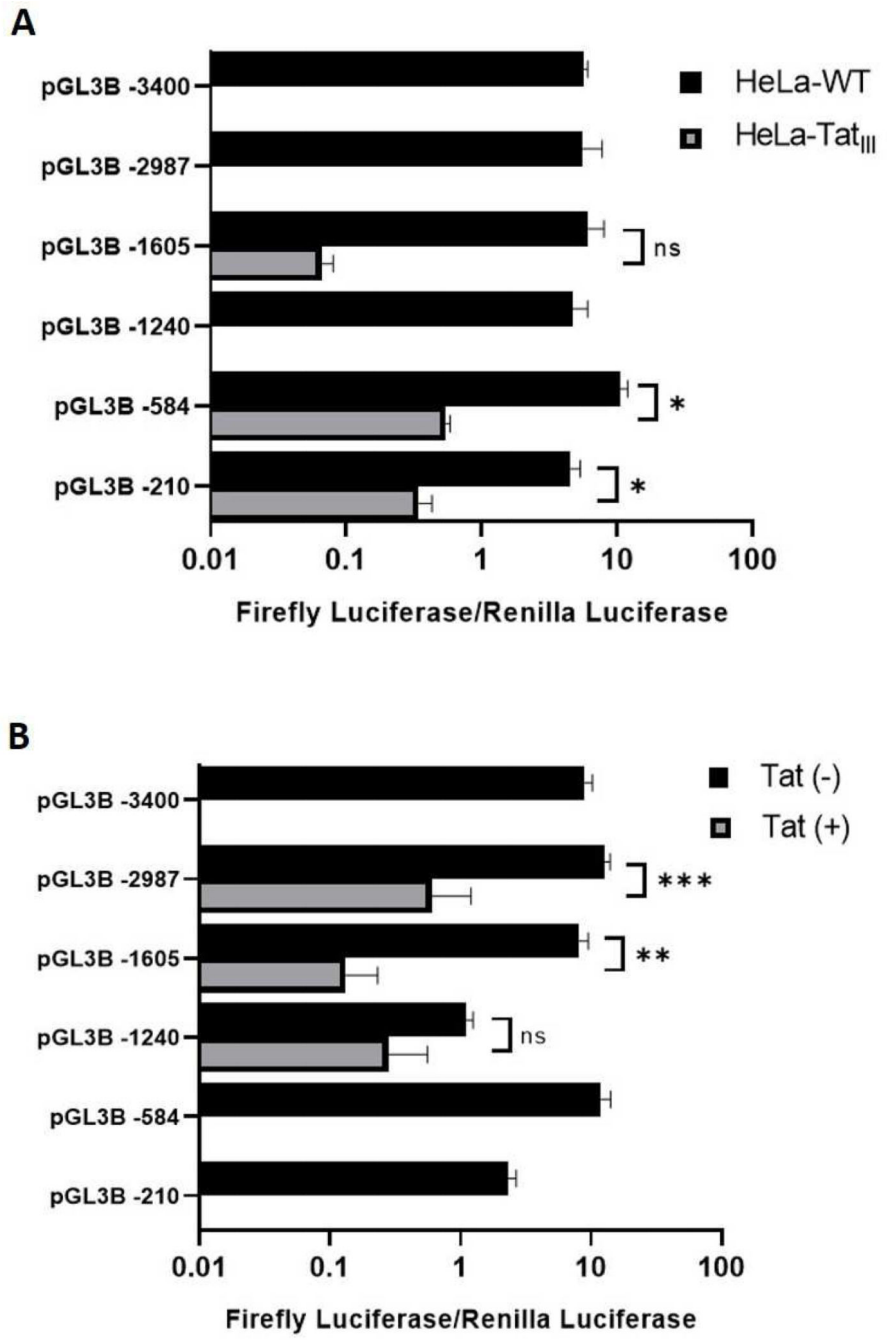

Figure 2. Tat represses expression from sod2 promoter reporters.

A) Expression from sod2- promoter-reporter constructs in HeLa-WT and stable HeLa transfectant that constitutively expresses the HIV Tat protein, HeLa-Tat$_{III}$. B) Expression from the sod2-promoter reporter constructs in HPAEC with (Tat(+)) and without (Tat(−)) co-transfection with pCP2-Tat. Firefly luciferase values were normalized to Renilla luciferase from co-transfected pRL-CMV plasmid. Shown is the Mean ± SEM of biological replicates, n ≥ 6, (*p ≤ 0.05, **p ≤ 0.01, ***p ≤ 0.001 by un-paired student's T-test).

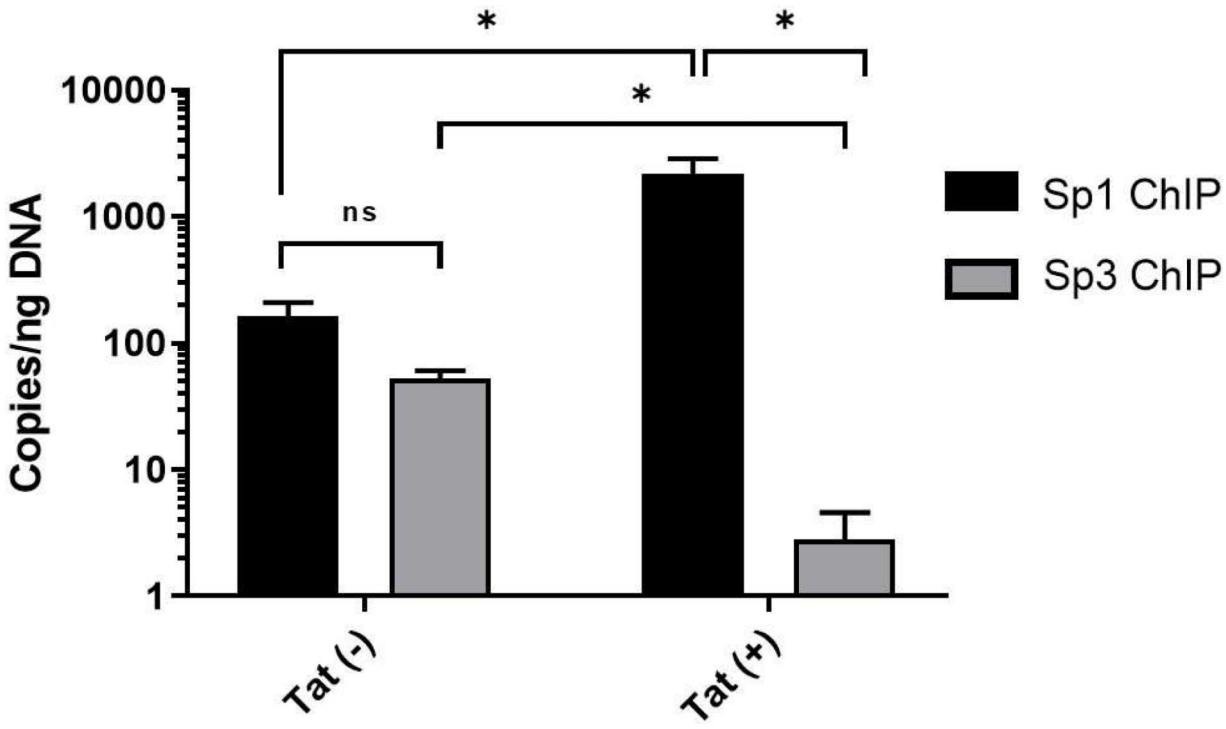

Figure 3. Chromatin immunoprecipitation (ChIP) analysis of Sp1 and Sp3 bound to the −584 region of the *sod2* promoter in un-transfected (Tat(−)) or pCP2-Tat_{101} transfected (Tat(+)) HPAEC.

Following IP with either Sp1 or Sp3 antibodies, the number of copies of the −584-nucleotide region of the endogenous *sod2* promoter was determined by absolute qPCR via a standard curve generated utilizing a plasmid containing −3406sod2-promoter sequences. n = 3. (*$p \leq 0.05$ by un-paired student's T-test). DNA that was immunoprecipitated using mouse IgG1 (serotype control) did not amplify.

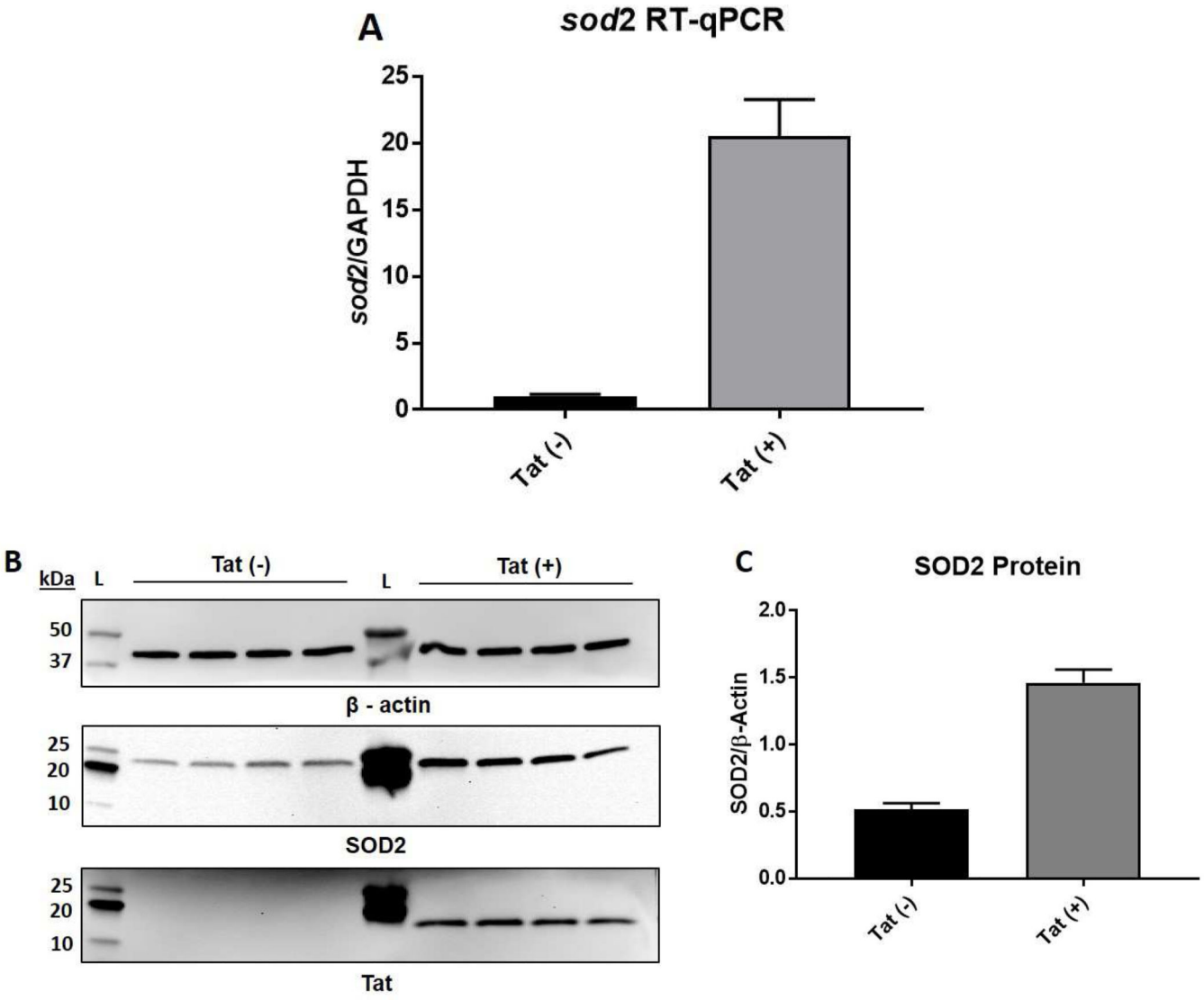

Figure 4. SOD2 expression in HPAEC in the presence and absence of Tat.

A) *sod2* transcription is strongly stimulated by HIV-Tat. Relative fold change calculated by the ΔΔCT method and normalized to GAPDH. Mean ± SEM of biological replicates, n= 6, $p < 0.0001$ by unpaired student's t-test. *B and C) SOD2 protein levels are increased in the presence of Tat.* Mean ± SEM of biological replicates, n= 4, ($p \leq 0.0001$ by unpaired student's t-test). SOD2 Densitometry values normalized to β-actin. L = MW ladder.

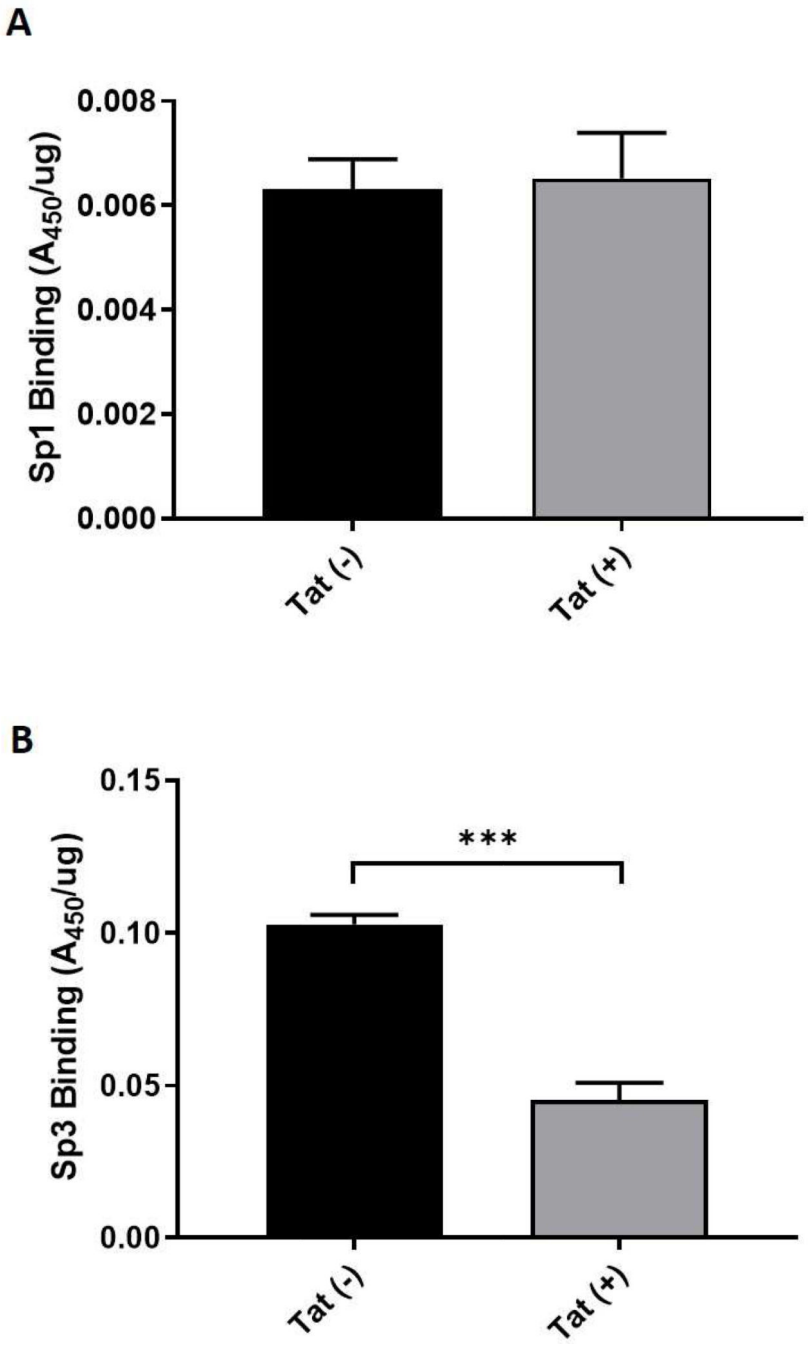

Figure 5. Sp1 and Sp3 Binding activity in HPAEC in the absence and presence of Tat.

Using an Sp-specific oligonucleotide-binding ELISA (TransAm, Active Motif), we measured the levels of active Sp1 (Panel A) and Sp3 (Panel B) in the nucleus of mock transfected (Tat(−)) or pCP2-Tat_{101} transfected (Tat(+)) HPAEC. The signal was normalized to μg of nuclear protein. Mean ± SEM of biological replicates, n = 3, (***$p \leq 0.001$ by unpaired student's T-test).

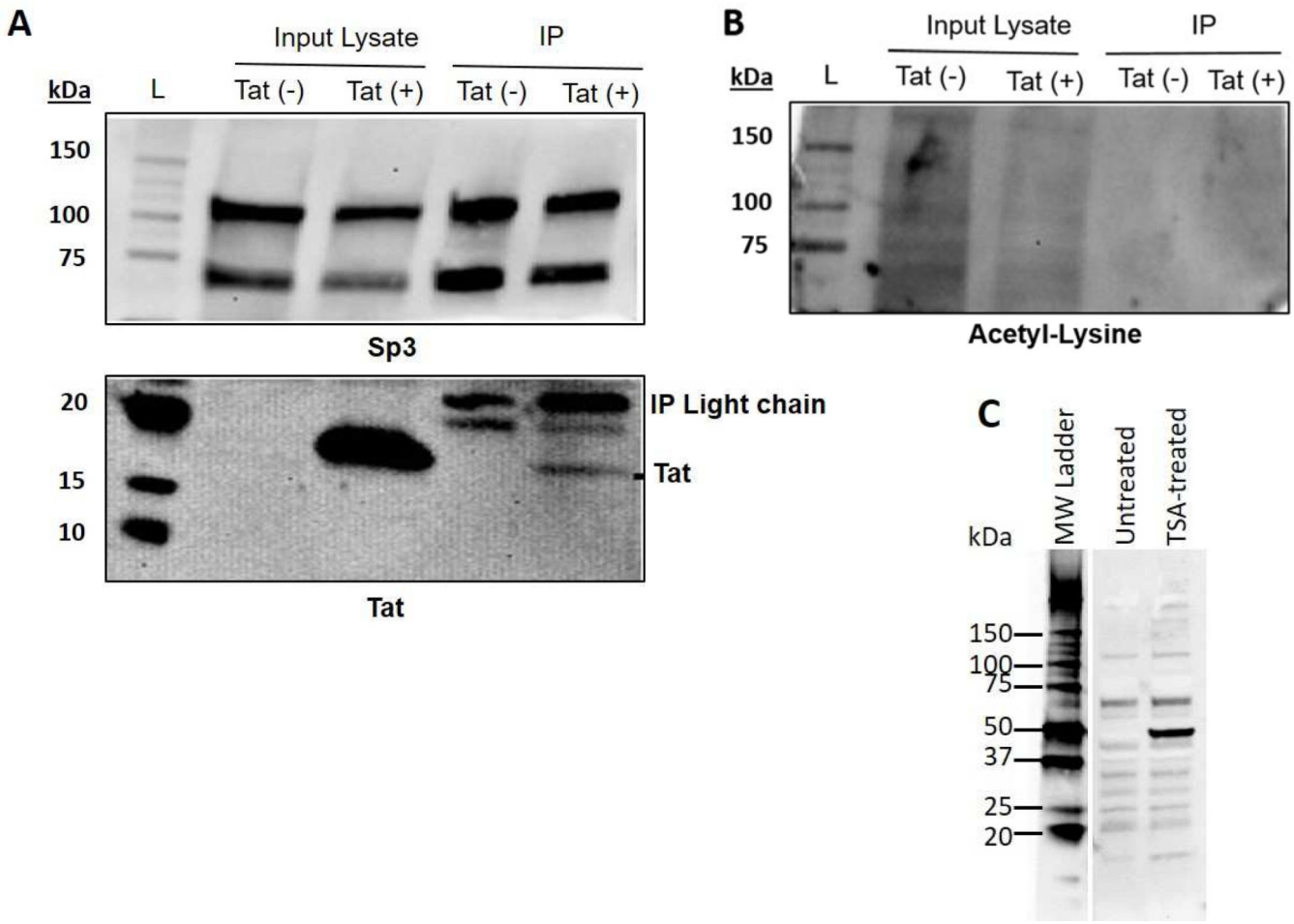

Figure 6. Tat Co-Immunoprecipitates with Sp3 but does not alter Sp3 acetylation State:

A) Sp3 and Tat Co-immunoprecipitate: Sp3 was immunoprecipitated from Tat (−) or Tat (+) HPAEC whole cell lysate. Total input lysate and immunoprecipitate were analyzed via immunoblot for successful Sp3 IP and potential Tat CoIP. *B) Sp3 acetylation state is not altered by interaction with Tat:* The total input lysate and Sp3 immunoprecipitate from Panel A was also analyzed via immunoblot with anti-acetyl-lysine antibodies. *C)* Acetyl lysine detection in the total protein lysates of Untreated or Trichostatin A (TSA) treated HPAEC.

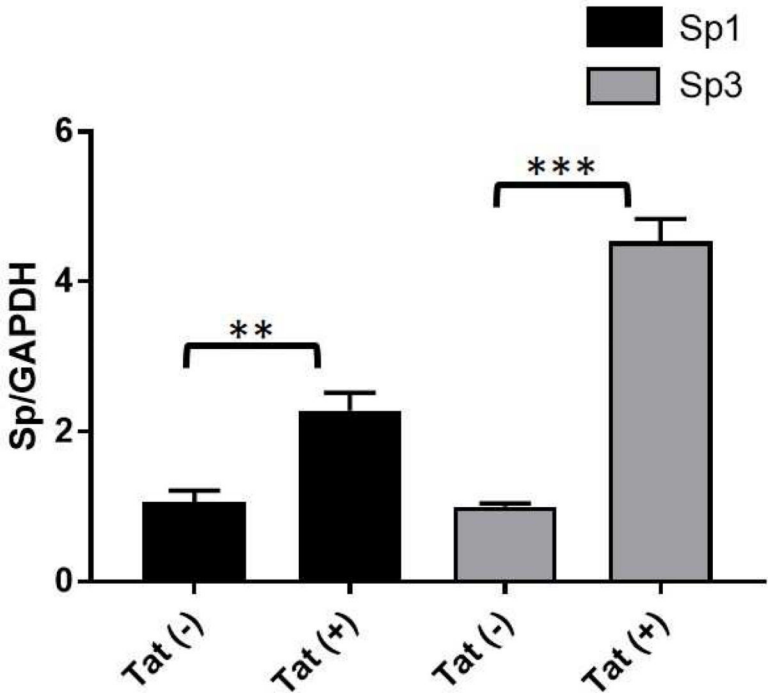

Figure 7. Transcription of Sp1 and Sp3 in the presence and absence of Tat in HPAEC.

A) Transcript levels of Sp1 and Sp3 in Tat (−) (mock transfected) and Tat (+) (pCP2-Tat$_{101}$-tranfected) HPAEC: Relative levels of transcript calculated by the ΔΔCT method and normalized to GAPDH (n = 6). Mean ± SEM of biological replicates (**p ≤ 0.01, ***p ≤ 0.001 by unpaired student's T-test).

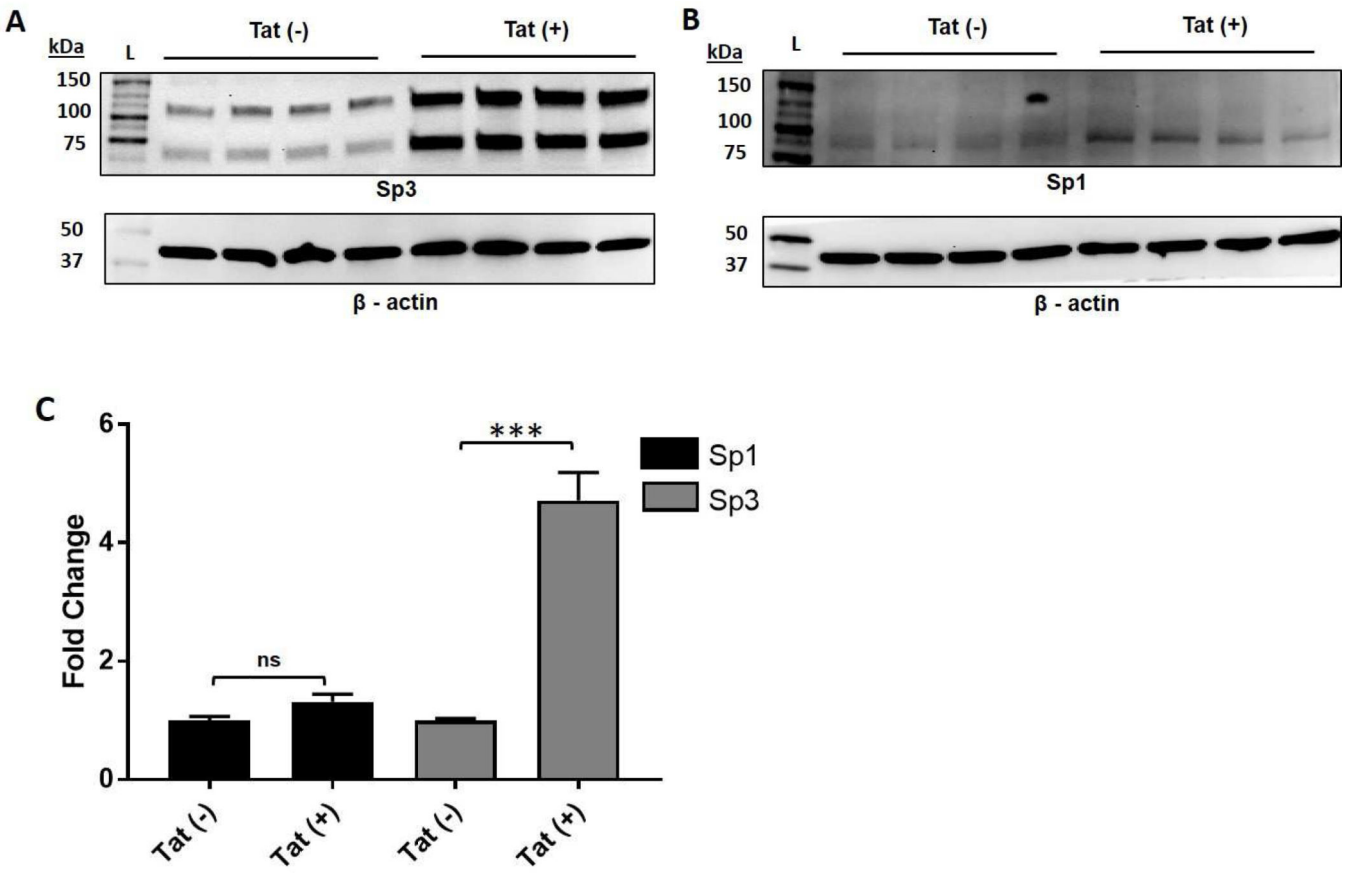

Figure 8. Sp1 and Sp3 protein levels in the absence and presence of Tat in HPAEC.

A-B) Sp3 and Sp1 expression is increased in Tat (+) HPAEC. Whole cell extract of mock transfected (Tat (−)) and pCP2-Tat_{101}-transfected (Tat (+)) HPAEC were analyzed via immunoblot for total levels of Sp3/Sp1. *C) Fold increase of Sp3 (top band) and Sp1 in Tat (+) and Tat (−) HPAEC.* Fold change in Sp expression was calculated as actin normalized Tat (+) densitometry values over actin normalized Tat (−) densitometry values (n = 4). Mean ± SEM of biological replicates L = MW ladder.

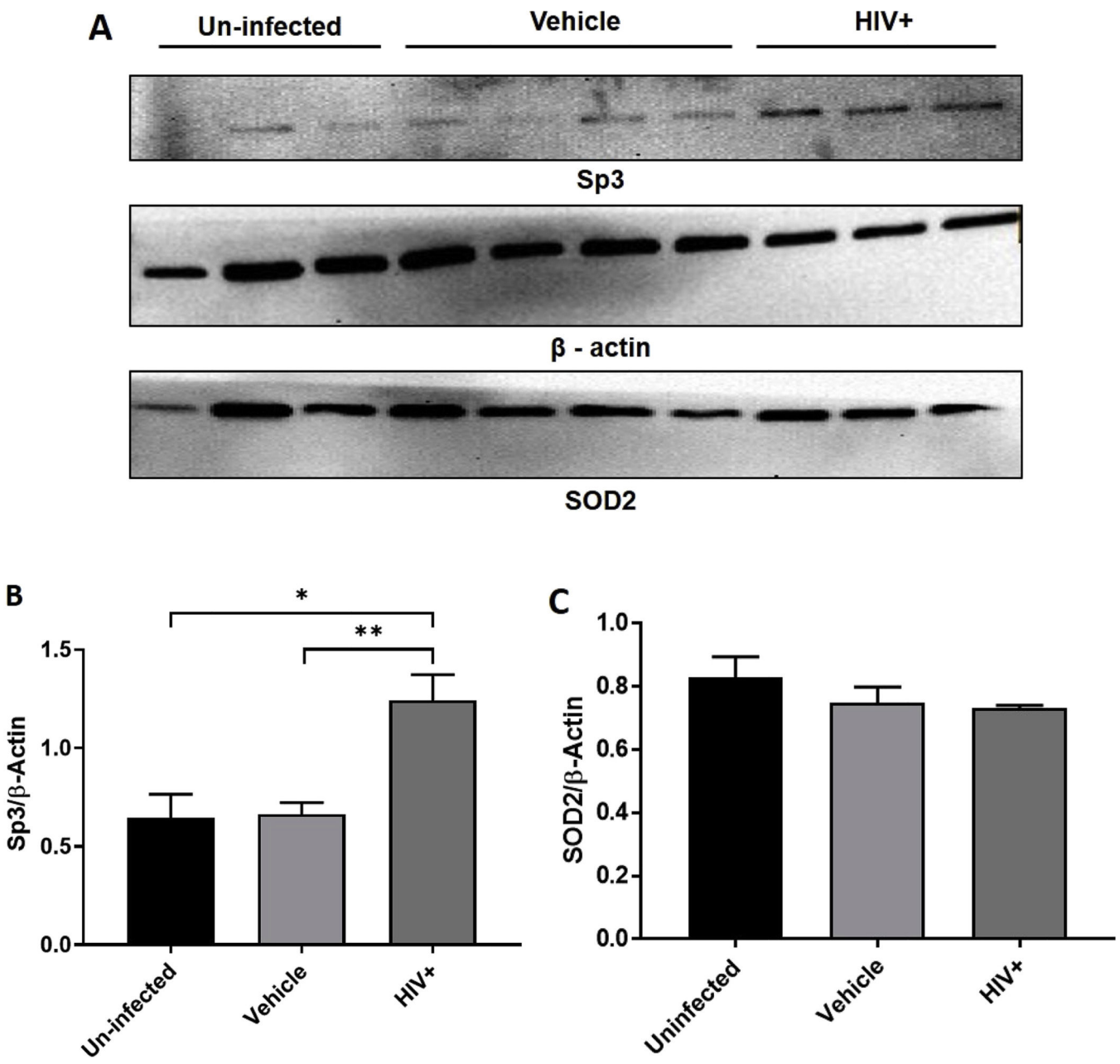

Figure 9. Sp3 expression increased in the Lungs of HIV infected mice while SOD2 did not change.

A) Immunoblot analysis of Sp3 and Sod2 levels in total lung tissue: Protein was extracted from whole lung tissue of un-infected, mock-infected, or HIV-1 infected humanized mice for immunoblot analysis. *B) Sp3 densitometry:* Values shown as normalized to β-actin. (un-infected n = 3, mock infected n = 4, HIV-1 infected n = 3). *C) Sod2 densitometry:* Values shown as normalized to β-actin. (un-infected n = 3, mock infected n = 4, HIV-1 infected n = 3). Mean ± SEM of biological replicates (*$p \leq 0.05$, **$p \leq 0.01$ by un-paired student's T-test).

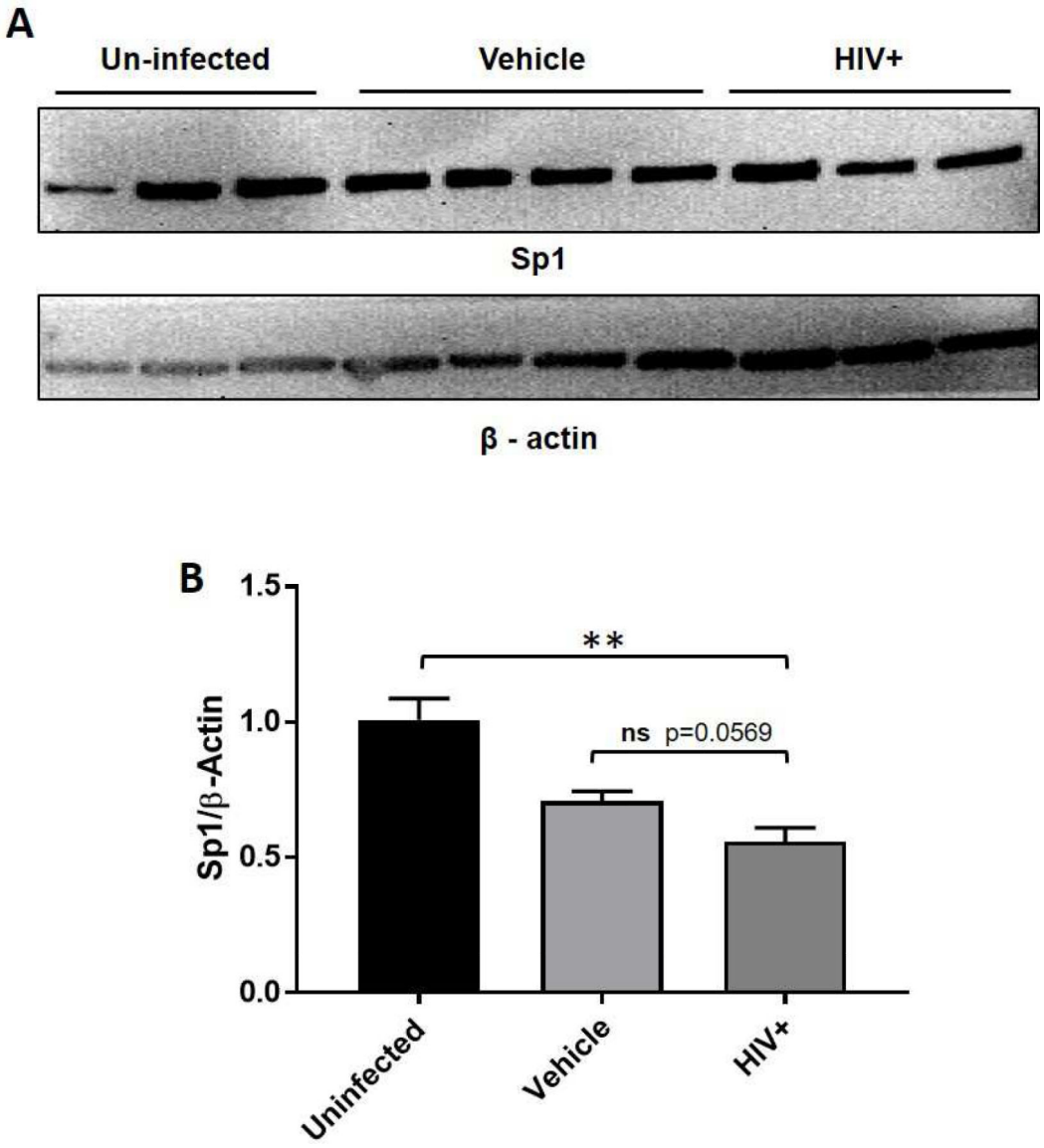

Figure 10. Sp1 expression in the Lungs of HIV infected mice.

A) Immunoblot analysis of Sp1 levels in total lung tissue of NSG-BLT Mice: Protein was extracted from whole lung tissue of un-infected, mock-infected, or HIV-1 infected humanized mice for immunoblot analysis. *B) Sp1 densitometry:* Values shown as normalized to β-actin. (un-infected n = 3, mock infected n = 4, HIV-1 infected n = 3). Mean ± SEM of biological replicates (**p ≤ 0.01 by un-paired student's T-test).

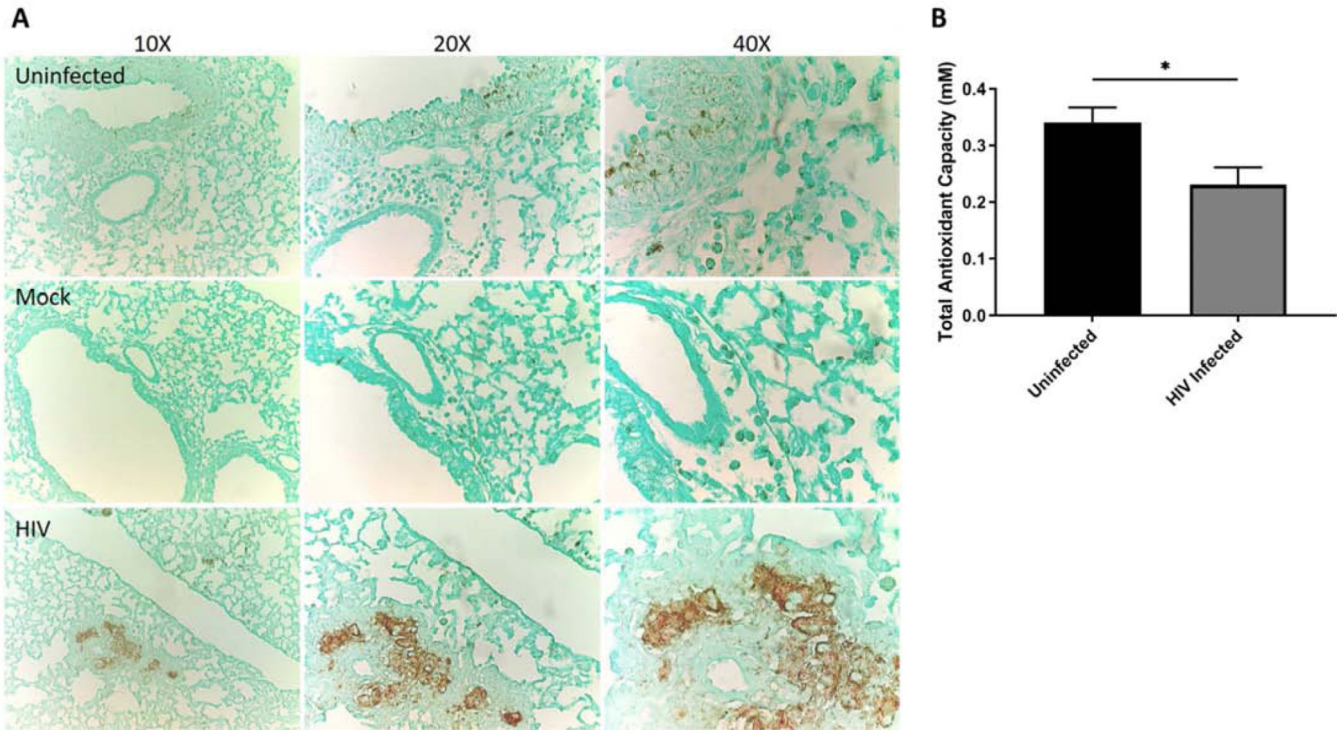

Figure 11. SOD2 levels are increased in the lungs of HIV infected humanized NSG-BLT mice while total antioxidant capacity is lower

A*)* IHC *of lung tissue from HIV infected (10 weeks) and uninfected humanized NSG-BLT mice reveals* periadventitial *increase in S0D2. B) Total antioxidant capacity (TAC) is reduced in the lungs of HIV infected humanized NSG-BLT mice (n = 8) compared to uninfected mice (n = 8). Mean ± SEM of biological replicates (*p ≤ 0.05 by un-paired student's T-test).*